NANO LETTERS

Letter

pubs.acs.org/NanoLett

Direct Modulation of Lanthanide Emission at Sub-Lifetime Scales

Sinan Karaveli, Aaron J. Weinstein, and Rashid Zia*

School of Engineering, Brown University, Providence, Rhode Island 02912, United States

Supporting Information

ABSTRACT: The long lifetime of lanthanide emitters can present a challenge for conventional pump-based modulation schemes, where the maximum switching speed is limited by the decay time of the excited state. However, spontaneous emission can also be controlled through the local optical environment. Here, we demonstrate a direct modulation scheme enabled by dynamic control of the local density of optical states (LDOS). Specifically, we exploit the LDOS differences between electric and magnetic dipole transitions near a metal mirror and demonstrate that rapid nanometer-scale mirror displacements can modulate the emission spectra of trivalent europium ions within their excited state lifetime. The dynamic LDOS modulation presented here can be readily extended to faster optical modulation schemes and applied to other long-lived emitters to control the direction, polarization, and spectrum of spontaneous emission at sublifetime scales.

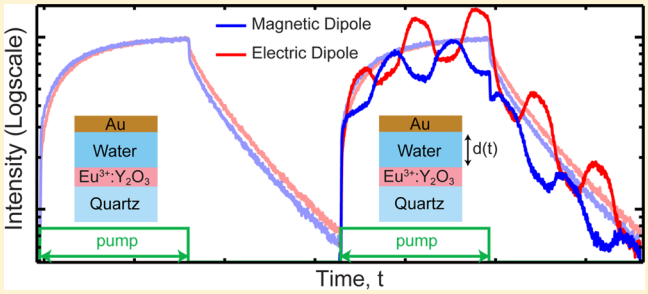

KEYWORDS: *Europium, lanthanides, local density of optical states (LDOS), magnetic dipole transitions, modulation, photoluminescence*

Trivalent lanthanide ions are important light emitters employed in many applications ranging from lighting and displays to lasers and optical telecommunication amplifiers. An important aspect of optical communication systems is the modulation of light to encode information. This is typically achieved by externally modulating the light from a laser, for example using a Mach−Zehnder interferometer,[1] but can also be achieved by directly modulating the excitation source of a laser[2] or light-emitting diode (LED).[3] Direct modulation of an LED could be desirable, especially for chip-scale integration,[4] because it can be simpler as well as more space- and energy-efficient than external modulation. It is often assumed that the direct modulation of a light source is limited by the spontaneous emission lifetime.[5] This is particularly problematic for lanthanide emitters as they have lifetimes on the order of milliseconds to hundreds of microseconds, which would restrict modulation speeds to the range of 1−10 kHz.

However, the spontaneous emission lifetime is not necessarily a fundamental limit. Erbium-doped silicon LEDs have been directly modulated faster than the intrinsic lifetime of erbium ions, up to speeds of 80 kHz, by quenching their emission with Auger processes.[6,7] Temporarily increasing the nonradiative decay rate $\Gamma_{nr}(t)$ helps to decrease the excited state lifetime and consequently turn off emission faster. This is similar to other excitation-based modulation schemes, where changes to the excitation rate $\Gamma_{exc}(t)$ are used to control the excited state population $N_{exc}(t)$ and thus the observed emission intensity: $I(t) \propto N_{exc}(t)\sum_i^{obs.}\Gamma^i_{rad}$, where Γ^i_{rad} is the radiative decay rate into the ith optical mode and the summation is taken over all the observed modes. For conventional excitation-based modulation, $\sum_i^{obs.}\Gamma^i_{rad}$ is essentially constant while the time-varying $N_{exc}(t)$ can be controlled by a variety of factors, as highlighted by the rate equation:[7] $(dN_{exc}/dt) = (N_0 - N_{exc})\Gamma_{exc} - (N_{exc}/\tau)$, where N_0 is the total number of excitable emitters and the excited state lifetime is $\tau = (\Gamma_{nr} + \sum_i^{all}\Gamma^i_{rad})^{-1}$. In this Letter, we demonstrate a proof-of-principle experiment for an alternative approach to achieve direct modulation of lanthanide emission. Rather than modulating the excited state population $N_{exc}(t)$, we modify the local optical environment and directly modulate the emission rate $\Gamma^i_{rad}(t)$ into different modes within the excited state lifetime.

It is well-known that an emitter's spontaneous emission depends both on its electronic states and the local density of optical states (LDOS) into which it may radiate.[8] Engineering the LDOS of an emitter is commonly employed to enhance or inhibit spontaneous emission. For example, by placing an emitter within an optical cavity[9] or near an optical antenna,[10] it is possible to enhance emission rates, direct radiation, and control polarization. Using surface acoustic waves to modify photonic crystal cavities, emission wavelengths have also been tuned at rates approaching the emitter lifetime.[11] More generally though, modifying the local optical environment can provide a way to modulate emission faster than the excited state lifetime. Once excited, an emitter's radiation depends only on its instantaneous LDOS; when it emits, it will radiate into the available optical modes at that point in time. Therefore, unlike pump-based modulation which is limited by the rise and fall

Received: March 8, 2013
Revised: April 15, 2013
Published: April 18, 2013

   dx.doi.org/10.1021/nl400883r | *Nano Lett.* 2013, 13, 2264−2269

time of the electronic state, dynamic optical control is fundamentally limited only by retardation effects.

To demonstrate modulation within the excited state lifetime, we tune the emission spectra of trivalent europium-doped yttrium oxide (Eu^{3+}:Y_2O_3) using a moving mirror. Eu^{3+} ions are long lifetime emitters exhibiting several electric dipole (ED) and magnetic dipole (MD) radiative transitions over visible wavelengths,[12] as shown in Figure 1a. In addition to recent

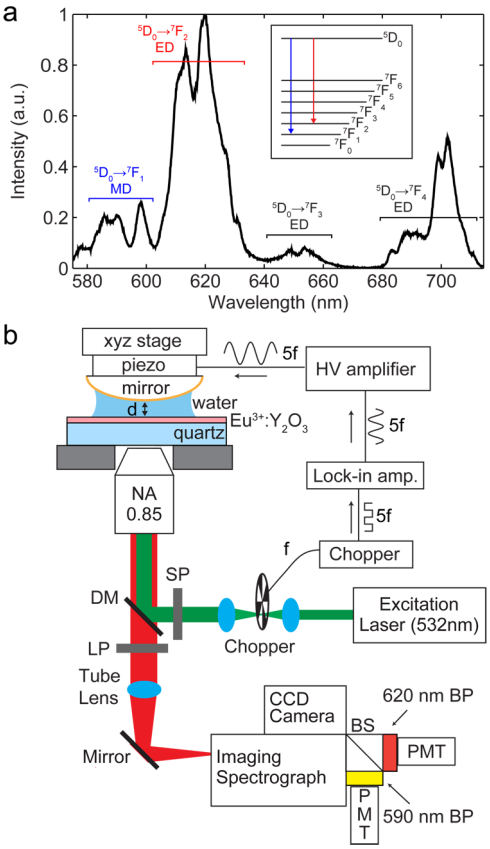

Figure 1. (a) Emission spectrum of 25 nm Eu^{3+}:Y_2O_3 thin film on quartz substrate highlighting the $^5D_0\rightarrow^7F_1$ MD transition and the $^5D_0\rightarrow^7F_2$ ED transition that are the focus of this study. Inset: Energy level diagram of Eu^{3+} showing the $^5D_0$ first excited state and the ^7F_J ground state manifold. (b) Schematic of the experimental setup. BP: band-pass filter, BS: beamsplitter, DM: dichroic mirror, f: chopper operating frequency, LP: long pass filter, PMT: photomultiplier tube, SP: short pass filter.

studies of MD emission,[13−15] these ions were used in the seminal experiments by Drexhage, Kunz, and Lukosz demonstrating lifetime variations near planar metal and dielectric surfaces.[16,17] The presence of a reflecting surface modifies the LDOS and, depending on its distance from the emitter, can either enhance or inhibit radiation.[18] Interestingly, within any inhomogeneous environment (e.g., near a planar interface), the electric and magnetic LDOS differ.[19] Due to self-interference effects, the LDOS for ED and MD transitions exhibit an inverse distance-wavelength dependence; namely for distances and wavelengths at which ED emission is enhanced, MD emission is inhibited and vice versa. We have previously used this LDOS difference to strongly enhance MD emission,[20] quantify ED and MD transitions,[21] and selectively tune between spectrally close ED and MD lines.[22] Here, we exploit the ED and MD transitions in Eu^{3+}:Y_2O_3 to unambiguously demonstrate dynamic LDOS-based emission modulation.

The luminescent sample was fabricated by cosputtering Eu_2O_3 and Y_2O_3 to deposit a 25 nm emitter layer of Eu^{3+}:Y_2O_3 on a quartz substrate, which was subsequently annealed at 1000 °C for 1 h. The moving mirror was made by evaporating a 10 nm Ti adhesion layer, 100 nm Au reflector layer, and 20 nm Y_2O_3 protection layer on a plano-convex lens with a 7.7 mm radius of curvature. This coated mirror was subsequently glued to a small piezoelectric actuator (Mad City Labs Inc., PZT1). The mirror-piezo assembly was mounted on a three-axis stage (see Figure 1b), which was used to center the mirror in the field of view of a 60×, 0.85 numerical aperture (NA) objective in an inverted microscope (Nikon, TE2000). The Newton ring interference fringes from the curved mirror surface were used to help align the system and ensure that the apex was centered on the excitation laser spot (532 nm, Coherent Verdi). A drop of deionized water was placed between the sample and mirror, increasing the refractive index; this directs more emission from the Eu^{3+} ions toward the mirror and thus enhances the LDOS modulation. The mirror was then slowly lowered toward the sample using the three-axis stage to a starting emitter-mirror distance less than 1 μm.

Using the piezoelectric actuator, the mirror was subsequently lowered toward the sample with 11.5 nm increments while acquiring the emission spectrum of Eu^{3+}:Y_2O_3 at each step. Figure 2a shows a color plot of the normalized emission spectra as a function of mirror displacement, Δd, from the starting position (see Supporting Information for a movie illustrating the dynamic modulation). To facilitate comparison, several of these spectra are plotted together in Figure 2b. Even for very small mirror displacements, the emission spectrum varies significantly. At $\Delta d = -195$ nm, the $^5D_0\rightarrow^7F_2$ ED transition (between 603 and 635 nm) dominates the emission spectrum, whereas at $\Delta d = -287$ nm, greater emission is observed from the $^5D_0\rightarrow^7F_1$ MD transition (between 580 and 603 nm).

The observed spectral variations in Figure 2a,b are consistent with previous experiments for separate Eu^{3+}:Y_2O_3 samples fabricated with different thickness emitter-mirror spacers and can be accurately predicted from the LDOS variations for ED and MD transitions at different wavelengths.[22] These transitions can be modeled as isotropic ED and MD emitters located within a planar four-layer structure, and the radiative decay rates Γ^{ED} and Γ^{MD} can be calculated using the self-interference formalism of Chance, Prock, and Silbey:[18]

$$\frac{\Gamma^{ED}}{\Gamma_0} = \frac{1}{2}\mathrm{Im}\left[\int_0^{u\max}\left(\frac{(1+R_{21}^p)(1+R_{23}^p)-2u^2(R_{21}^p+R_{23}^p)}{1-R_{21}^pR_{23}^p} + \frac{(1+R_{21}^s)(1+R_{23}^s)}{1-R_{21}^sR_{23}^s}\right)\frac{u\,du}{l_2}\right] \quad (1)$$

$$\frac{\Gamma^{MD}}{\Gamma_0} = \frac{1}{2}\mathrm{Im}\left[\int_0^{u\max}\left(\frac{(1-R_{21}^s)(1-R_{23}^s)+2u^2(R_{21}^s+R_{23}^s)}{1-R_{21}^sR_{23}^s} + \frac{(1-R_{21}^p)(1-R_{23}^p)}{1-R_{21}^pR_{23}^p}\right)\frac{u\,du}{l_2}\right] \quad (2)$$

where $R_{21}^{s,p} = \{r_{21}^{s,p} + [t_{21}^{s,p}t_{12}^{s,p}r_{10}^{s,p}\exp(-2kl_1d)]/[1 - r_{12}^{s,p}r_{10}^{s,p}\exp(-2kl_1d)]\}\exp(-2kl_2s_{21})$ and $R_{23}^{s,p} = r_{23}^{s,p}\exp(-2kl_2s_{23})$ are based on the reflection and transmission coefficients for *s*- and *p*-polarization: $r_{i,j}^s = (l_i - l_j)/(l_i + l_j)$, $r_{i,j}^p = (\varepsilon_i l_j - \varepsilon_j l_i)/(\varepsilon_i l_j + \varepsilon_j l_i)$, $t_{ij}^s = 2l_i/(l_i + l_j)$, and $t_{ij}^p = 2l_i(\varepsilon_i\varepsilon_j)^{1/2}/(\varepsilon_j l_i + \varepsilon_i l_j)$. d is the distance between the emitting film and the mirror. s_{ij} is the distance of

dx.doi.org/10.1021/nl400883r | Nano Lett. 2013, 13, 2264−2269

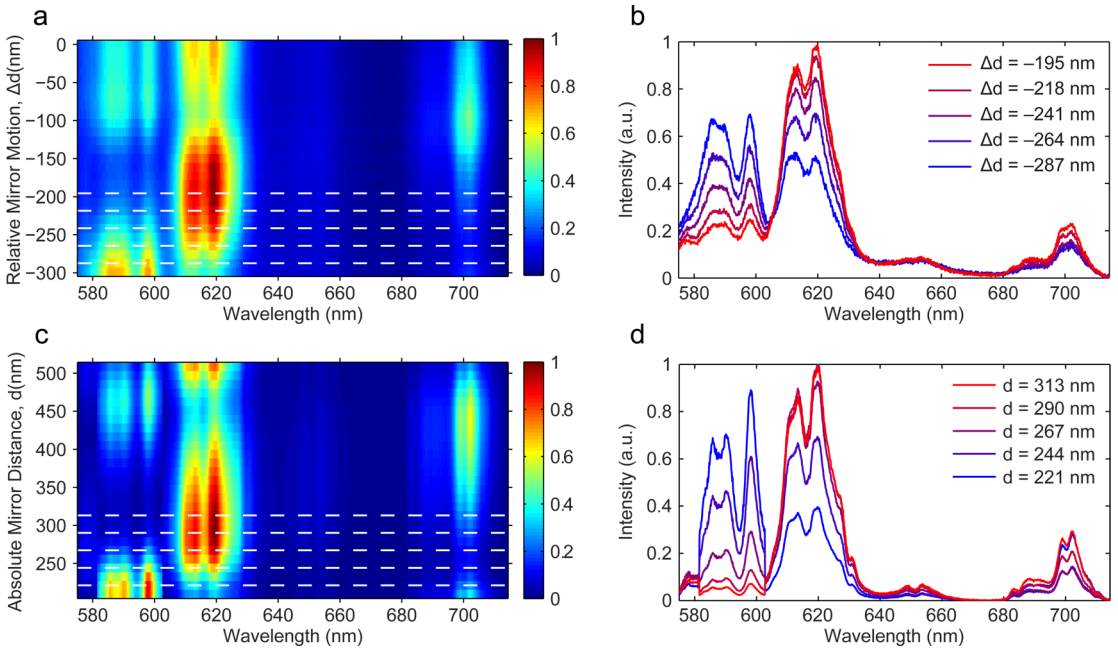

Figure 2. Comparison of experimental (a–b) and theoretical (c–d) normalized emission spectra as a function of mirror position. (a) Experimental emission spectra as a function of the relative displacement Δd measured as the mirror was lowered toward the sample. Dashed white lines indicate positions of the spectra plotted together in b. (c) Calculated emission spectra as a function of absolute emitter-mirror distance d. Dashed white lines indicate positions of the spectra plotted together in d.

the emitter from the i,j interface. $u = k_{\|}/k$ and $l_j = -i(n_j^2/n_2^2 - u^2)^{1/2}$ are the parallel and perpendicular components of the wavevector normalized to the emitter layer wavenumber, $k = (2\pi/\lambda)n_2$. Here, the subscript indices 0, 1, 2, and 3, respectively, represent the gold mirror, water (n_1 = 1.33), Eu^{3+}:Y_2O_3 (n_2 = 1.78), and quartz substrate (n_3 = 1.46) layers. The dispersive refractive index of gold (n_0) was modeled by the Brendel–Bormann model.[23] For simplicity, we assume that the emitters are located at the center of the 25 nm Eu^{3+}:Y_2O_3 layer (i.e., $s_{21} = s_{23}$ = 12.5 nm) and subsume the optical effects of the thin Y_2O_3 mirror coating into the adjacent water layer. Γ_0 is the intrinsic emission rate in a homogeneous medium with index n_2.

Integrated to infinity, $u_{max} = \infty$, eqs 1 and 2 describe the total radiative rate for ED and MD transitions into all modes and thus incorporate the total electric and magnetic LDOS respectively. These equations can also be used to calculate the modified emission rate into a subset of modes, that is, the partial LDOS. Specifically, setting $u_{max} = NA/n_2$ allows us to calculate the modified radiation rate into the collection NA of our objective for different emitter-mirror separation distances, d. As the observed emission intensity at each wavelength and mirror position is proportional to the radiative rate into the collected optical modes, $I(\lambda,d) \propto \Gamma_{rad}(\lambda,d)$, eqs 1 and 2 can be used to calculate a normalized emission spectrum: $I_N(\lambda,d) \equiv I(\lambda,d)/\int I(\lambda,d)d\lambda = \Gamma_{rad}(\lambda,d)/\int \Gamma_{rad}(\lambda,d)d\lambda$, where $\Gamma_{rad}(\lambda,d)$ is either $\Gamma^{ED}(\lambda,d)$ or $\Gamma^{MD}(\lambda,d)$. We have previously shown that a reference emission spectrum obtained for a known optical environment, $I_N(\lambda,d_{ref})$, can be used to predict the normalized emission spectra at different positions using:[22]

$$I_N(\lambda, d) = \frac{I_N(\lambda, d_{ref})\Gamma_{rad}(\lambda, d)/\Gamma_{rad}(\lambda, d_{ref})}{\int I_N(\lambda, d_{ref})\Gamma_{rad}(\lambda, d)/\Gamma_{rad}(\lambda, d_{ref})d\lambda} \quad (3)$$

Figure 2c shows the theoretical spectra calculated for a range of emitter–mirror distances. These spectra were obtained with eq 3 by using the normalized spectrum acquired from the bare sample prior to water and mirror addition (Figure 1a) as a reference. Note that there is good agreement between the experimental data and the theoretical spectra. Matching the calculated and measured spectra also allows us to estimate the emitter–mirror distance, and thus relate the relative displacement Δd of the open-loop piezoelectric actuator to an absolute distance d. Despite the introduction of large background signals from both the water and the gold mirror in the experimental measurements, the predicted spectra in Figure 2d capture the dominant changes observed in the Eu^{3+} emission lines.

The strong dependence on mirror position seen in Figure 2 can be leveraged to rapidly direct Eu^{3+} emission into either the ED $^5D_0 \rightarrow {}^7F_2$ or MD $^5D_0 \rightarrow {}^7F_1$ transition. Using the piezoelectric actuator, the mirror is first brought to a height where the ratio of ED to MD emission changes strongly for small mirror displacements. Then, a 10 kHz sinusoidal voltage signal is applied to the piezo, causing the mirror to move up and down. While continuously pumping the ions with the excitation laser, MD and ED emission was simultaneously monitored using two photomultiplier tubes (Hamamatsu H7422-40P) with different band-pass filters covering the wavelength ranges of 585–595 nm and 605–635 nm, respectively. Figure 3 shows the intensity modulation as a function of time and thus mirror position. As expected from Figure 2 and the LDOS variations, light emission from the ED and MD transitions are inversely correlated. Every 50 μs, the observed emission intensity shifts back and forth between ED and MD. However, unlike the normalized spectra in Figure 2, the observed intensity signals themselves can be difficult to interpret for a number of reasons. First and foremost, in addition to modifying the emission of the Eu^{3+} ions, the mirror motion also changes the pump intensity at the ions' location and thus their excitation rate; consequently, the observed intensity variations may be the product of both excitation and emission modulation. As discussed earlier, there

dx.doi.org/10.1021/nl400883r | Nano Lett. 2013, 13, 2264–2269

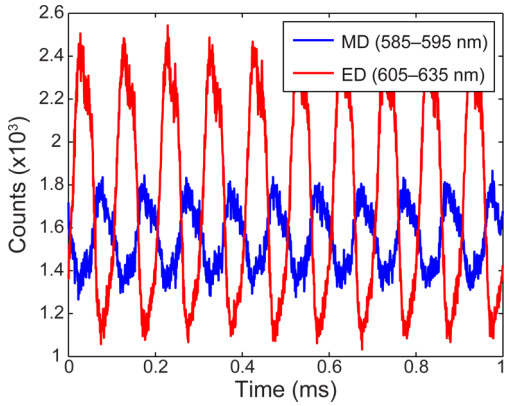

Figure 3. Time-resolved fluorescence observed during dynamic LDOS modulation for continuous-wave excitation. The mirror is dithered at 10 kHz, while the Eu^{3+} emission is observed with two PMTs with band-pass filters covering 585−595 nm and 605−635 nm ranges corresponding to the $^5D_0 \rightarrow {}^7F_1$ MD and $^5D_0 \rightarrow {}^7F_2$ ED transitions, respectively.

is also background luminescence from both the water and the gold mirror.

To demonstrate that the observed effect is a result of LDOS modification to Eu^{3+} emission, and not an artifact of background or pump variations, we performed pulsed-excitation time-resolved experiments. First, keeping the mirror position fixed, the pump laser is modulated with a mechanical chopper (Stanford Research Systems, SR540) at a frequency of 1.5 kHz. Figure 4a shows that, after an initial fast decay attributed to background fluorescence, both the ED and MD emission exhibit a slow single exponential decay corresponding to a ∼108 μs lifetime for the $^5D_0$ excited state (108.9 ± 1.2 μs fit for the ED data, 107.2 ± 1.2 μs fit for the MD data). Next, the position of the mirror was varied using a sinusoidal voltage synchronized to 5 times the mechanical chopper speed (mirror operating frequency, 7.5 kHz). Similar to Figure 3, inverse oscillations were observed in the ED and MD emission intensities during the pumping period (see Figure 4b). Note though that, even after the laser excitation ends, the ED and MD transitions continue to exhibit an inverse relationship, clearly demonstrating that the observed modulation is not an artifact of pump variations. Furthermore, the observed modulation on the decay for both ED and MD emission is faster than the excited state lifetime. The transitions exhibit oscillations from high to low emission every ∼67 μs, and five relative extrema are clearly observed after the pump signal ends. The recovery of the multiple ED and MD emission peaks during the decay together with their inverse oscillations indicate that quenching of emission due to the gold mirror does not play a significant role. Such near-field quenching effects are important when the emitter is very close to the metal surface, but their effects are negligible for the large (>200 nm) emitter-mirror separation distances used in this study.

The modulation observed in Figure 4b can be accurately described by the same theoretical framework used to predict the emission spectrum at different mirror positions shown in Figure 2. To this end, we assume that the emitter−mirror separation distance varies sinusoidally with time: $d(t) = d_a \sin(2\pi f t) + d_0$, where f is the mirror operation frequency (7.5 kHz), d_a is the amplitude of the mirror motion, and d_0 is the center position about which the mirror oscillates. For each distance value, a normalized emission spectrum can be

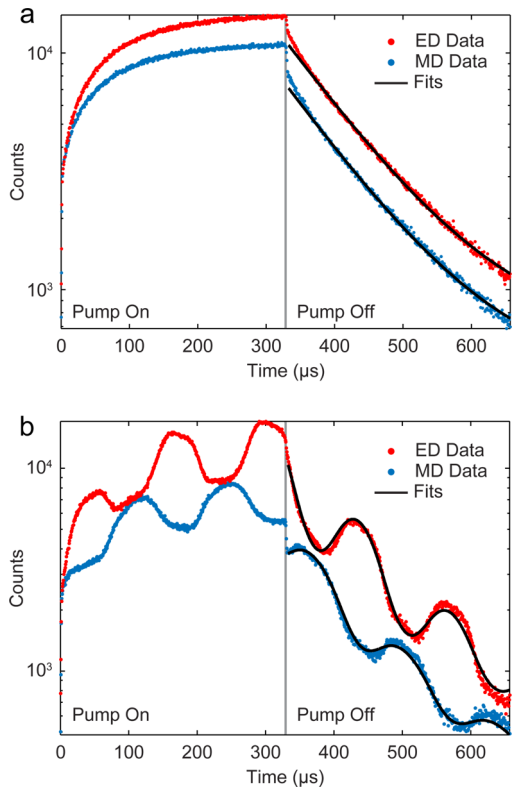

Figure 4. Pulsed-excitation time-resolved photoluminescence measurements of the ED and MD emission. Vertical gray lines indicate when the pump laser pulse ends. (a) Experimental time-traces of the ED (605−635 nm) and MD (585−595 nm) emission, red and blue dots respectively, for fixed mirror position. Single exponential fits (black lines) confirm that both transitions arise from the same excited state with a ∼108 μs lifetime; fit lifetimes are 108.9 ± 1.2 μs and 107.2 ± 1.2 μs, respectively, for the ED and MD emission. (b) Experimental time-traces of the ED and MD emission obtained when the mirror is dithered at 7.5 kHz highlighting their inverse oscillations both during and after pulse excitation. Multiple oscillations observed on the decay after the pump ends are clear evidence of dynamic modulation within the excited state lifetime and are consistent with the theoretical fits (black lines) obtained using eq 4.

calculated and integrated over the wavelength ranges corresponding to the two bandpass filters. Assuming that the excited state lifetime remains constant, the time varying integrated intensity can be calculated as:

$$I(t) = \left(\int_\lambda \frac{I_N(\lambda, d(t))}{I_N(\lambda, d_0)} d\lambda \right) I_0 e^{-t/\tau} + C \tag{4}$$

where the excited state lifetime τ = 108 μs and the detector dark counts C are obtained from fits to the fixed mirror position data in Figure 4a. I_0 is the observed intensity at the start time for the fit (t = 0). The best match to the experimental data is obtained for d_0 = 249 nm and d_a = 16 nm, indicating that the observed modulation results from nanometer scale displacement of the mirror position. Furthermore, this agreement between the experimental results and eq 4 also indicates that the observed modulation results primarily from changes in the ED and MD emission rates, while the total radiative rate of the $^5D_0$ excited state remains relatively constant. Finally, note that the optical phase shift resulting from such small displacements can readily be achieved at significantly higher speeds. In these experiments, the LDOS was varied using the mechanical

dx.doi.org/10.1021/nl400883r | Nano Lett. 2013, 13, 2264−2269

motion in water of a macroscopic mirror mounted to a piezoelectric actuator, and therefore, the maximum modulation speed was limited by the mechanical resonance of the mirror-piezo assembly and drag induced coupling with the sample surface. Faster LDOS modulation could be achieved through other mechanical schemes, for example, using integrated piezoelectric or electrostrictive thin films,[24] or any technique that can modulate the refractive index, for example, through field- or carrier-induced[25] electro-optic effects or using phase change materials.[26,27]

In conclusion, we have shown a proof-of-principle experiment demonstrating the sublifetime modulation of emission through dynamic control of the local optical environment. These results highlight that the excited state lifetime does not impose a fundamental limit on modulation speeds. Even with a constant excited state population (e.g., a saturated steady-state ensemble of emitters), emission can still be tuned at sublifetime speeds by varying the local optical environment. In such a system, light will be continuously emitted, but control over the LDOS can determine into which modes (defined by momentum, polarization, and wavelength) light is emitted. Here, we have focused specifically on wavelength variations in Eu^{3+}, because of the stark differences in the LDOS for its spectrally distinct ED and MD transitions near a simple mirror. With this system, it was possible to observe variations even when collecting emission from a large set of radiation modes. The observed modulation could be significantly greater in a well-designed optical waveguide or cavity,[28] where ED and MD variations would be enhanced, and emission would be primarily directed into a finite number of cavity modes. Such methods can be readily extended to other lanthanide ions exhibiting strong MD transitions,[29] including trivalent erbium (Er^{3+}). In addition to spectral control, dynamic LDOS modulation can also be used to tailor the direction[30] and/or polarization of light emission, which could be especially useful for directing the emission of on-chip Er^{3+} LEDs into different waveguide modes. Finally, the optical modulation methods presented here can also work for any transition, whether ED or MD in nature, and therefore are applicable to other long-lived emitters, including silicon nanocrystals.[31]

■ ASSOCIATED CONTENT

Supporting Information

Movie illustrating the dynamic modulation of the normalized emission spectra as a function of mirror position based on the experimental data shown in Figure 2a. This material is available free of charge via the Internet at http://pubs.acs.org.

■ AUTHOR INFORMATION

Corresponding Author

*E-mail: rashid_zia@brown.edu.

Notes

The authors declare no competing financial interest.

■ ACKNOWLEDGMENTS

The authors thank S. Cueff, C. M. Dodson, M. Jiang, J. Kurvits, D. Li, and D. Pacifici for helpful discussions. Financial support for this work was provided by the Air Force Office of Scientific Research (PECASE award FA-9550-10-1-0026) and the National Science Foundation (CAREER award EECS-0846466).

■ REFERENCES

(1) Liu, A.; Jones, R.; Liao, L.; Samara-Rubio, D.; Rubin, D.; Cohen, O.; Nicolaescu, R.; Paniccia, M. A high-speed silicon optical modulator based on a metal-oxide-semiconductor capacitor. *Nature* **2004**, 615−618.

(2) Fang, A. W.; Kock, B. R.; Jones, R.; Lively, E.; Liang, D.; Kuo, Y.-H.; Bower, J. E. A distributed Bragg reflector silicon evanescent laser. *IEEE Photon. Technol. Lett.* **2008**, *20*, 1667−1669.

(3) Shambat, G.; Ellis, B.; Majumdar, A.; Petykiewicz, J.; Mayer, M. A.; Sarmiento, T.; Harris, J.; Haller, E. E.; Vučković, J. Ultrafast direct modulation of a single-mode photonic crystal nanocavity light-emitting diode. *Nat. Commun.* **2011**, *2*, 539.

(4) Fan, P.; Colombo, C.; Huang, K. C. Y.; Krogstrup, P.; Nygård, J.; Fontcuberta i Morral, A.; Brongersma, M. L. An electrically-driven GaAs nanowire surface plasmon source. *Nano Lett.* **2012**, *12*, 4943−4947.

(5) Ramaswami, R.; Sivarajan, K. N.; Sasaki, G. H. *Optical Networks: A Practical Perspective; Elsevier/Morgan Kaufmann*, 3rd ed.; Morgan Kaufmann: Burlingon, MA, 2009; pp 192−193.

(6) Coffa, S.; Franzò, G.; Priolo, F. High efficiency and fast modulation of Er-doped light emitting Si diodes. *Appl. Phys. Lett.* **1996**, *69* (14), 2077−2079.

(7) Franzò, G.; Coffa, S.; Priolo, F.; Spinella, C. Mechanism and performance of forward and reverse bias electroluminescence at 1.54 μm from Er-doped Si diodes. *J. Appl. Phys.* **1997**, *81*, 2784−2793.

(8) Purcell, E. M. Spontaneous emission probabilities at radio frequencies. *Phys. Rev.* **1946**, *69*, 681.

(9) Vahala, K. J. Optical microcavities. *Nature* **2003**, *424*, 839−846.

(10) Curto, A. G.; Volpe, G.; Taminiau, T. H.; Kreuzer, M. P.; Quidant, R.; van Hulst, N. F. Unidirectional Emission of a Quantum Dot Coupled to a Nanoantenna. *Science* **2010**, *329*, 930.

(11) Fuhrmann, D. A.; Thon, S. M.; Kim, H.; Bouwmeester, D.; Petroff, P. M.; Wixforth, A.; Krenner, H. J. Dynamic modulation of photonic crystal nanocavities using gigahertz acoustic phonons. *Nat. Photon.* **2011**, *5*, 605−609.

(12) Freed, S.; Weissman, S. I. Multipole nature of elementary sources of radiation − wide-angle interference. *Phys. Rev.* **1941**, *60*, 440−442.

(13) Noginova, N.; Zhu, G.; Mavy, M.; Noginov, M. A. Magnetic dipole based systems for probing optical magnetism. *J. Appl. Phys.* **2008**, *103*, 07E901.

(14) Noginova, N.; Barnakov, Y.; Li, H.; Noginov, M. A. Effect of metallic surface on electric dipole and magnetic dipole emission transitions in Eu3+ doped polymeric film. *Opt. Express* **2009**, *17*, 10767−10772.

(15) Ni, X.; Naik, G. V.; Kildishev, A. V.; Barnakov, Y.; Boltasseva, A.; Shalaev, V. M. Effect of metallic and hyperbolic metamaterial surfaces on electric and magnetic dipole emission transitions. *Appl. Phys. B: Laser Opt.* **2011**, *103*, 553−558.

(16) Drexhage, K. H. Interaction of light with monomolecular dye layers. *Prog. Optics* **1974**, *12*, 163−232.

(17) Kunz, R. E.; Lukosz, W. Changes in the fluorescence lifetimes induced by variable optical environments. *Phys. Rev. B* **1980**, *21*, 4814−4828.

(18) Chance, R. R.; Prock, A.; Silbey, R. Molecular fluorescence and energy transfer near interfaces. *Adv. Chem. Phys.* **1978**, *37*, 1−65.

(19) Joulain, K.; Carminati, R.; Mulet, J.-P.; Greffet, J.-J. Definition and measurement of the local density of electromagnetic states close to an interface. *Phys. Rev. B* **2003**, *68*, 245405.

(20) Karaveli, S.; Zia, R. Strong enhancement of magnetic dipole emission in a multilevel electronic system. *Opt. Lett.* **2010**, *35*, 3318.

(21) Taminiau, T. H.; Karaveli, S.; van Hulst, N. F.; Zia, R. Quantifying the Magnetic Nature of Light Emission by Energy Momentum Spectroscopy. *Nat. Commun.* **2012**, *3*, 979.

(22) Karaveli, S.; Zia, R. Spectral Tuning by Selective Enhancement of Electric and Magnetic Dipole Emission. *Phys. Rev. Lett.* **2011**, *106*, 193004.

(23) Rakic, A. D.; Djurišic, A. B.; Elazar, J. M.; Majewski, M. L. Optical properties of metallic films for vertical-cavity optoelectronic devices. *Appl. Opt.* **1998**, *37*, 5271−5283.
(24) Kingon, A. I.; Srinivasan, S. Lead zirconate titanate thin films directly on copper electrodes for ferroelectrics, dielectric and piezoelectric applications. *Nat. Mater.* **2005**, *4*, 233−237.
(25) Feigenbaum, E.; Diest, K.; Atwater, H. A. Unity-order index change in transparent conducting oxides at visible frequencies. *Nano Lett.* **2010**, *10*, 2111−2116.
(26) Cavalleri, A.; Tóth, C.; Siders, C. W.; Squier, J. A.; Ráksi, F.; Forget, P.; Kieffer, J. C. Femtosecond structural dynamics in VO_2 during an ultrafast solid-state phase transition. *Phys. Rev. Lett.* **2001**, *87*, 237401.
(27) Briggs, R. M.; Pryce, I. M.; Atwater, H. A. Compact silicon photonics waveguide modulator based on the vanadium dioxide metal-insulator phase transition. *Opt. Express* **2010**, *18*, 11192−11201.
(28) Ameling, R.; Giessen, H. Cavity plasmonics: large normal mode splitting of electric and magnetic particle plasmonics induced by a photonic microcavity. *Nano Lett.* **2010**, *10*, 4394−4398.
(29) Dodson, C. M.; Zia, R. Magnetic dipole and electric quadrupole transitions in the trivalent lanthanide series: Calculated emission rates and oscillator strengths. *Phys. Rev. B* **2012**, *86*, 125102.
(30) Chen, Y.; Lodahl, P.; Koenderink, A. F. Dynamically reconfigurable directionality of plasmon-based single photons sources. *Phys. Rev. B* **2010**, *82*, 081402.
(31) Carreras, J.; Arbiol, J.; Garrido, B.; Bonafos, C.; Montserrat, J. Direct modulation of electroluminescence from silicon nanocrystals beyond radiative recombination rates. *Appl. Phys. Lett.* **2008**, *92*, 091103.